FLYWCH1, a Novel Suppressor of Nuclear β-catenin, Regulates Migration and Morphology in Colorectal Cancer

Belal A. Muhammad[1,2≠], Sheema Almozyan[1≠], Roya Babaei-Jadidi[1≠], Emenike K. Onyido[1], Anas Saadeddin[1,3], Seyed Hossein Kashfi[1], Bradley Spencer-Dene[4,5], Mohammad Ilyas[6], Anbarasu Lourdusamy[7], Axel Behrens[8] and Abdolrahman S. Nateri[1*]

[1] Cancer Genetics and Stem Cell Group, Cancer Biology, Division of Cancer and Stem Cells, [6] Molecular Pathology Unit, [7] Children's Brain Tumour Research Centre, School of Medicine, University of Nottingham, Nottingham NG7 2UH, UK.

[2] Division of Experimental Haematology and Cancer Biology, Cincinnati Children's Hospital Medical Centre, Cincinnati, OH 45229, USA.

[3] Tres Cantos Medicines Development Campus, GlaxoSmithKline, Calle de Severo Ochoa, 2, 28760 Tres Cantos, Madrid, Spain.

[4] Experimental Histopathology Laboratory, the Francis Crick Institute, London NW1 1AT, UK

[5] Advanced Cell Diagnostics, UK

School of Medicine, Queen's Medical Centre, University of Nottingham, NG7 2UH UK

[8] Adult Stem Cell Laboratory, the Francis Crick Institute, London NW1 1AT, UK.

[≠] Co-first authors

Running title: FLYWCH1/β-catenin Axis Regulates Cell Migration

*****Correspondence to: Abdolrahman S. Nateri, a.nateri@nottingham.ac.uk

Tel: 0044-115-8231306

Fax: 0044-115-8231137

Conflict of interest: The authors declare that they have no conflict of interest.

Abstract

Wnt/β-catenin signaling plays a critical role during development of both normal and malignant colorectal cancer (CRC) tissues. Phosphorylation of β-catenin protein alters its trafficking and function. Such conventional allosteric regulation usually involves a highly specialized set of molecular interactions, which may specifically turn on a particular cell phenotype. This study identifies a novel transcription modulator with an FLYWCH/Zn-finger DNA-binding domain, called "FLYWCH1". Using a modified yeast-2-hybrid based Ras-Recruitment system, it is demonstrated that FLYWCH1 directly binds to unphosphorylated (nuclear) β-catenin efficiently suppressing the transcriptional activity of Wnt/β-catenin signaling that cannot be rescued by TCF4. FLYWCH1 rearranges the transcriptional activity of β-catenin/TCF4 to selectively block the expression of specific downstream genes associated with CRC cell migration and morphology, including ZEB1, EPHA4, and E-cadherin. Accordingly, overexpression of FLYWCH1 reduces cell motility and increases cell attachment. The expression of FLYWCH1 negatively correlates with the expression level of ZEB1 and EPHA4 in normal versus primary and metastatic CRC tissues in patients. Thus, FLYWCH1 antagonizes β-catenin/TCF4 signaling during cell polarity/migration in CRC.

Implications: This study uncovers a new molecular mechanism by which FLYWCH1 with a possible tumor suppressive role represses β-catenin-induced ZEB1 and increases cadherin-mediated cell attachment preventing colorectal cancer metastasis.

Keywords

Colorectal cancer (CRC)/Migration/Metastasis/β-catenin /FLYWCH1/Wnt-signalling

Introduction

Activated Wnt-signalling has significant implications both in cellular homeostasis and carcinogenesis depending on the context of activation and the surrounding microenvironment. Accumulated evidence identified several proteins that interact with nuclear-β-catenin and antagonise its transcriptional activity leading to transcriptional repression of Wnt-target genes. Accordingly, any alterations of the Wnt/β-catenin pathway through β-catenin corepressors is often involved in crucial biological processes ranging from normal development to cancer. For instance, Sox9 regulates the progression of the chondrocyte differentiation pathway during endochondral bone formation through inhibition of β-catenin (1), whereas the Wnt-signalling attenuator RUNX3 was proposed to function as a tumour suppressor during intestinal tumourigenesis (2). Moreover, expression of Chibby, a nuclear-β-catenin associated antagonist of the Wnt/Wingless pathway, was also linked to embryonic development and cancer (3). These findings indicate that β-catenin co-repressors function as potential gate-keepers for the activity of β-catenin, ensuring that a proper threshold of β-catenin is achieved before its interaction with members of T-cell factor (TCF) and lymphoid enhancer factor (LEF) transcription factors (TCF/LEFs).

Furthermore, the paradox of β-catenin/TCF interaction, however, is challenged by identification of new strategies for β-catenin-dependent but TCF-independent gene regulation. It has been reported that β-catenin interacts with Prop-1 rather than members of TCFs to regulate the cell-lineage determination during pituitary gland development (4). β-catenin was also found to control the pluripotency of embryonic-stem cells through interaction and enhancement of Oct-4 activity independently of TCFs (5). Likewise, the involvement of several other DNA-binding transcription factors with β-catenin was reported in the literature. Some are enhancing the promoter binding ability of β-catenin and facilitate the chromatin remodelling at the promoter site of Wnt-target genes such as p300/CBP and Brg-1(6, 7), while others are promoting nuclear-localisation of β-catenin such as Pygopus (8). Corepressors such

as ICAT (inhibitor of β-catenin and TCF4) and p15RS antagonize Wnt-signalling through inhibiting the interaction and formation of β-catenin/TCF4 complex (9). Moreover, RUNX3 forms a ternary complex with β-catenin/TCF4 by which attenuates Wnt-signalling activity (2). Similar to this mechanism, RAR, Chibby, Sox-9, and HIF-1α compete with members of TCF/LEF for binding to β-catenin (1, 3, 10, 11).

Notably, some of the β-catenin-binding transcription factors including KLF4, Glis2/3, HIC1, and Osx belong to the Cys2-His2 (C_2H_2) family of Zinc-finger proteins characterised by having multiple C_2H_2-type Zinc-finger DNA-binding domains (12-15). These proteins could potentially regulate the gene expression programs controlled by Wnt/β-catenin-signalling via their interaction with β-catenin and/or TCFs, disrupting the formation of β-catenin/TCF-complexes, and subsequently recruiting nuclear-β-catenin to the promoter of specific target genes independently of TCFs. However, this view of nuclear-β-catenin recruitment has not yet been fully explored.

To further delineate the nuclear events of the Wnt-signalling pathway, we employed a modified yeast two-hybrid Ras-Recruitment System (RRS) using mouse embryonic-cDNA library and identified several new proteins that bind β-catenin in a GSK-3β phosphorylation-dependent and/or independent manner. One of the proteins was FLYWCH1, a conserved nuclear protein containing multiple FLYWCH-type zinc-finger domains with unknown function. FLYWCH motif has first been described and annotated based on the presence of FLYWCH consensus sequence (**F**/Y–Xn–**L**–Xn–F/**Y**–Xn–**W**XCX$_{6\text{-}12}$**C**X$_{17\text{-}22}$HX**H**; where X indicates any amino acid) in *Drosophila* (16, 17). In addition, FLYWCH motifs were also identified and studied in two more proteins of *C. elegans*: PEB-1 (18) and FLYWCH transcription factors; FLH-1, FLH-2, and FLH-3 (19). Based on *Drosophila* and *C. elegans* studies, FLYWCH motifs may function in protein-protein interactions and serve as DNA-

binding domains (16-19). Accordingly, it can be predicted that human FLYWCH1 may have similar biological activities. However, no evidence for the presence of a transactivation-domain within the coding region of this protein was detected. To further characterise FLYWCH1, we set out to functionally describe its interaction with β-catenin and explore its importance and role(s) in colorectal cancer (CRC).

Materials and Methods

Human tissues

49 CRCs tissues were arrayed on a TMA block in triplicates by the Molecular Pathology Unit from the consenting patients through the Nottingham tissue bank, as described previously (20).

Antibodies

Antibodies were purchased as follow: β-catenin (610154, BD-Transduction and 9582, Cell-Signalling), ZEB2/SIP1 (H260, Santa-Cruz), Vimentin (RV202, Santa-Cruz), ZEB1 (H-102 and E-20X, Santa-Cruz), E-cadherin (BD-Biosciences), TCF4 (Upstate; 05-511), FLYWCH1 (Sigma; HPA040753, Santa-Cruz; V18), GFP (3E6, Invitrogen), Flag-tag (F1804, Sigma), Myc-tag (9E10, Millipore) and β-Actin (Abcam).

Plasmids

The IMAGE-clone of human *FLYWCH1*-cDNA purchased from Geneservice (ID: 4839062/AK34; GenBank: 84256). Human FLYWCH1 gene is composed of 2,151 nucleotides encoding a protein with 716aa residues called FLYWCH1. The IMAGE-clone

plasmid DNA then digested with several restriction-enzymes and cloned into different vectors, while fused with the MYC-tag, His6, and eGFP. The FLAG-β-catenin^{WT}, FLAG-β-catenin^{S35A}, FLAG-β-catenin$^{S33A,\ S37A,\ T41A,\ S45A}$, TCF4, human *c-jun*-promoter-Luc, TOP/FOP-FLASH-Luc reporters previously described (21, 22). The –1129/+55 of *ZEB*1-promoter-Luc was from Dr M. Saito (Tokyo, Japan), FLAG-GSK-3β-plasmid was from Prof B.W. O'Malley (Houston, USA) and the packaging plasmids were kindly provided by Dr D. Bonnet (London, UK). pEGFP-C2 was purchased from Clontech, pBluescript-SK (Stratagene), pcDNA3.1 (Invitrogen), pET-His6, pGEX-KT (Addgene), the scrambled piLenti-scrambled control shRNA (scs)-GFP and piLenti-FLYWCH1-set-shRNA-GFP (set of 4) from ABM Inc (https://www.abmgood.com/FLYWCH1-shRNA-Lentivectors-i008000.html).

Modified yeast-2-hybrid based Ras-recruitment system (RRS)

The RRS uses the growth defective yeast strain cdc25-2, which is deficient in Ras activity and cannot grow at 37°C (23). Briefly, the yeast cells stably transformed with p*MET*3-GSK-3β then co-transformed with a bait composed of the FLAG-tagged construct of β-catenin lacking the 7-8 armadillo-domains (ΔARM) and fused to oncogenic RasV12 (RasV12-FLAG-β-catenin/ΔARM). Furthermore, the expression of GSK-3β and substrate-phosphorylation dependency is dependent on the presence (*promoter*-off) and absence (*promoter*-on) of methionine in yeast. Thus, the activated-GSK-3β (under the control of a *methionine*-regulated *MET*3-promoter) induces phosphorylation of FLAG-β-catenin–ΔARM. These cells then transformed with mouse embryonic-cDNA library fused to the Src-myristylation signal (Stratagene). Glucose plates were grown for 5 days at 25ºC then plated onto minimal

galactose plates (+/–methionine) at a restrictive temperature 36-37ºC. Yeast colonies exhibiting efficient methionine-dependent growth isolated and further analyzed.

In-situ hybridization (ISH) assay

Both sense and anti-sense *FLYWCH*1 RNA-probes generated by cloning a short nucleotide sequence of human *FLYWCH*1-cDNA into a pcDNA3 (details can be provided upon request). Both probes transcribed with *T7*-RNA polymerase using DIG-RNA-labelling mix (Roche) and ISH-assay carried out through the core facility at the CRUK-LRI as described previously (24).

Immunofluorescence (IF) assay

For IF, CRC cell-lines were grown on coverslips, fixed for 30mins with 4%paraformaldehyde and permeabilised with 0.5%Triton-X100 in PBS. Samples were exposed to goat anti-rabbit antibodies conjugated to Alexa-Fluor594 (A11037, Invitrogen) and/or rabbit anti-mouse antibodies conjugated to Alexa-Fluor488 (A11059, Invitrogen). Tetramethylrhodamine-B isothiocyanate (TRITC) conjugated Phalloidin (P1951, Sigma) used to label actin filaments according to manufacturer's instruction. Finally, slides mounted in Vectashield-DAPI medium (Vector Labs) and analysed by fluorescent microscopy.

Transient and stable cell transfections

Human CRCs (HCT116, DLD-1 and SW480), TIG119 fibroblasts and HEK293T cells maintained in RPMI supplemented with 10%FBS. Cells transiently transfected using Lipofectamine-2000 (Invitrogen). After 48hrs, cells processed for transcriptional analysis, mRNA or protein extraction. SW480 cells stably knocked-down for FLYWCH1 by lentiviral

transduction of piLenti-FLYWCH1-set-shRNA-GFP and control piLenti-scsRNA- (scrambled control shRNA) GFP. Both cells selected in a Puromycin-containing medium for 2-weeks then the resistant cells trypsinised, counted and seeded into 96-well plates (one cell/well). Finally, the resistant colonies derived from a single-seeded cell further amplified and expanded. The knocked-down status of FLYWCH1 validated through RT-PCR and IF analysis. R-spondin1 (293T-HA-Rspo1-Fc) and Wnt-3a (293T-HA-L) expressing cell-lines were a gift from Prof Hans Clevers (Hubrecht, Netherlands). R-spondin1/Wnt-3a conditioned media validated by a TOP/FOP-flash luciferase-reporter assay before using it.

Western-blot (WB), Immunoprecipitation (IP) and Chromatin-immunoprecipitation (ChIP) assays

We performed WBs and IPs as previously described (25, 26). For *in-vitro* binding assays, cDNAs encoding FLAG-β-catenin, and GFP-FLYWCH1 were translated by a T7-*in-vitro*-coupled transcription/translation system (Promega). λ-phosphatase (BioLab) treatment was carried out with 200units for 60mins at 30^{o}C. Immunocomplexes were captured by rotating for 2-3hrs with protein-A, Protein-G (Sigma) or secondary pre-coated Dynal-magnetic beads. In some cases, conjugated Agarose beads were used. Immunoprecipitates washed four-times with lysis buffer, and SDS-PAGE separated sample proteins then transferred onto PVDF-membranes (Amersham) following standard procedures. ChIP analysis performed as described previously (20, 21).

Competition assay

Recombinant human β-catenin protein 1ug/ml (Abcam), was used to coat a 96 well ELISA plate overnight at 4ºC. The plate was washed x3 with PBS-T and then blocked 2hrs at room

temperature. For the TCF4-detection/ calibration curve; after three washes, TCF4 recombined protein (Autogen Bioclear) added to the plate (range: 0.0 - 500ng) and incubated at 37ºC for 6hrs. The plate was washed x3 PBS-T and incubated with 2µg/ml of TCF4-FITC (Autogen Bioclear) for 1hr at room temperature. Following washing with PBS-T (x3) 50ul PBS was added. The level of fluorescent was estimated in a fluorescence microplate reader green setting excitation 494nm and emission 518nm. For the FLYWCH1-detection/ calibration curve; after 3x washes, FLWYCH1 recombined protein (Sigma) added to the plate (range: 0.0 - 500 ng). Plate incubated at 37ºC for 6hrs, and after three washes with PBS-T, 2µg/ml of FLYWCH1-HRP (Sigma) added to the wells and incubated 1hr at room temperature. The plate washed with PBS-T (x3). TMB (Tetramethylbenzidine) reagent A and B mixed and 100µL of mixed solution transferred to each well and incubated at 37°C for 20min. 50µL of TMB stop solution was added to each well and absorbance read at OD (450nm) in the microplate reader. The experiment for secondary antibodies interaction have been carried out, and there was no significant difference observed. Next, based on the calibration curve, TCF-4 100ng/ml and FLWYCH1 80ng/ml and mixer of both proteins added to wells already coated with human β-catenin protein (each triplicate). The plate incubated at 37ºC for 6hrs and after three washes with PBS-T incubated with 2µg/ml of TCF4-FITC. The plate incubated for 1hr at room temperature and washed with PBS-T and added 50µl PBS and read in fluorescence microplate reader green setting excitation 494nm and emission 518nm.

Electrophoretic mobility shift assays (EMSA)

For studying DNA-protein interactions, we used the LightShift Chemiluminescent EMSA kit (Thermo Scientific) that uses a non-isotopic method to detect DNA-protein interactions. Biotin end-labelled DNA contains 3x of *Tcf*-DNA-binding site incubated with SW480 nuclear

protein extract in the absent and/or present of recombinant TCF4 and FLYWCH1 proteins as outlined above. This reaction is then subjected to gel electrophoresis on a native polyacrylamide gel. The biotin end-labelled DNA is detected using the streptavidin-horseradish peroxidase conjugate and the chemiluminescent substrate according to the manufacturer's protocol (Thermo Scientific).

Luciferase assay

A firefly reporter gene (TOP-FLASH) driven by three copies of *Tcf*-binding elements (*ATCAAAG*) upstream to *TK*-minimal-promoter (which is specifically regulated by Wnt/β-catenin signalling) was used. Luciferase-activity measured using the Dual-Luciferase system (Promega) as described (20). For statistical analysis, the ratio of Firefly-Luc activity was normalised to *Renilla*-Luc. Data were expressed as fold-induction from three independent experiments.

Cell spreading, migration and wound healing assays

CRC cells synchronised in G0-phase of the cell cycle by serum-free starvation for 18hrs before cell motility assays. Electric cell-substrate impedance-sensing (ECIS) system was used for cell attachment and spreading assays in a confluent layer, according to manufacturer's guidelines. The system was run for 24hrs after which the quantification data of cell attachment and spreading was collected. Cell migration and wound healing assays assay were performed as previously described (24). All assays were performed at least three times in triplicate.

RT-PCR and quantitative RT-PCR assays

We extracted total RNA from homogenised primary-tumours and cultured cells using Trizol (Sigma) or RNeasy purification kit (Qiagen). Superscript-III First-strand synthesis (Invitrogen) and oligo(dT) primers were used to convert the RNA to cDNA according to the manufacturer's instructions. qPCR was accomplished with SYBR-green (Roche), and the data were analysed using LightCycler-480 software (Roche) and primers below.

```
5′-AGGTGACAGCATTGCTTCTG       (forward: β-actin)
5′-AGGGAGACCAAAGCCTTCAT       (reverse: β-actin)
5′-GTCTGTAGGAAGGCACAGCCTGTCG (forward: CDH1)
5′-AGGACCAGGACTTTGACTTGAGC    (reverse: CDH1)
5′-GCTGGAGGTCTGCGAGGA         (forward: CCND1)
5′-CATCTTAGAGGCCACGAACA       (reverse: CCND1)
5′-AGAAGGTGTGGGCAGAAGAA       (forward: CD44)
5′-AAATGCACCATTTCCTGAGA       (reverse: CD44)
5′-ACCCCAAGATCCTGAAACAG       (forward: c-Jun)
5′-ATCAGGCGCTCCAGCTCG         (reverse: c-Jun)
5′-AAAACCAGCAGCCTCCCGC        (forward: c-Myc)
5′-GGCTGCAGCTCGCTCTGC         (reverse: c-Myc)
5′-GGCAAGCATGAGACTGTGAA       (forward: ENFB1)
5′-ACTCCAAGGTGGCATTGTTC       (reverse: ENFB1)
5′-CTGCTGGATCAACCAGGAAT       (forward: ENFB2)
5′-TCTAGCACAGACGGCAACAG       (reverse: ENFB2)
5′-AGGATTACCCTGTGGTGGTC       (forward: EPHB2)
5′-TACAACGCCACAGCCATAAA       (reverse: EPHB2)
5′-TCGTGGTCATCGCTATCGTCT      (forward: EPHB3)
5′-AAACTCCCGAACAGCCTCATT      (reverse: EPHB3)
5′-CGACAAAGAGCGTTTCATCA       (forward: EPHA4)
5′-GCTTCACCCAAGTGGACATT       (reverse: EPHA4)
5′-GCAAAGGTCGAAGACCAGGA       (forward: FLYWCH1)
5′-TTCCTGGTGTACGAGTCCTT       (reverse: FLYWCH1)
5′-GGAGACCGACCAGGAGAC         (forward: FSCN1)
5′-CATTGGACGCCCTCAGTG         (reverse: FSCN1)
5′-GACAACAGCAGTATGGACG        (forward: LGR5)
5′-GCATTACAAGTAAGTGCCAG       (reverse: LGR5)
5′-GGCATACACCTACTCAACTACGG    (forward: ZEB1)
5′-TGGGCGGTGTAGAATCAGAGTC     (reverse: ZEB1)
5′-AATGCACAGAGTGTGGCAAGGC     (forward: ZEB2)
5′-CTGCTGATGTGCGAACTGTAGG     (reverse: ZEB2)
```

Statistical analysis

The significance of differences between mean and median was determined using the Student's *t*-test and the Mann-Whitney *U* test, as appropriate. Significance testing was performed using SPSS version 15. Mean ± SD (*, $P < 0.05$; **, $P < 0.01$; ***, $P < 0.001$) values are shown.

Results

FLYWCH1 and its physical interaction with β-catenin

FLYWCH1 is an uncharacterized protein product of the human *FLYWCH*1 gene. The sequence of this gene is publicly available (http://www.ncbi.nlm.nih.gov/gene/84256), yet its function remained undefined. The first evidence of FLYWCH1/β-catenin interaction comes from our large-scale screening using a modified yeast-2-hybrid based RRS (Fig 1, A-C) (23). As the bait, we used the FLAG-tagged construct of β-catenin lacking the 7-8 armadillo-domains (ΔARM) (FLAG-β-cateninΔARM) to avoid any interaction with TCF/LEF and other known nuclear proteins (Fig 1B). The expression of GSK-3β and substrate-phosphorylation dependency is dependent on the presence (*promoter*-off) and absence (*promoter*-on) of methionine in yeast (Fig 1C). This RRS utilizes an embryonic cDNA library (pMyr-cDNA library). Thus, cdc25-2 mutant yeasts can grow at 37°C, when a phosphorylation-dependent and independent interaction between a protein target and RasV12-β-cateninΔARM takes place. Therefore, to determine GSK-3β phosphorylation-independent interactions between human β-catenin and myristoylated target proteins, yeast colonies exhibiting efficient methionine-dependent growth isolated and further analyzed. The β-cateninΔARM(bait)-dependent growth of these clones was further analyzed on galactose-containing medium at 37°C. This screening allowed us to identify several proteins that specifically bound to unphosphorylated-β-catenin (Table S1). The FLYWCH1 protein contains a tandem array of five FLYWCH-type Zinc-finger motifs (Fig 1, D-E) and a putative nuclear localisation signal (NLS) motif (KRAK, Fig S1A) closely resembling the classical NLS motif consensus

sequences (K-R/K-X-K/R). We tested multiple antibodies from various commercial sources, unfortunately despite a lot of efforts no commercial antibody can detect the endogenous FLYWCH1 protein in Western-blotting (WB) and immunoprecipitation (IP), while working on immunofluorescence (IF) assays. Therefore, the full-length cDNA of human *FLYWCH*1 tagged with MYC-epitope (MYC-FLYWCH1) or eGFP (GFP-FLYWCH1) were used for biochemical/molecular analyses (WB, IP, Co-IP, etc.) in this study.

To confirm our initial screening data regarding FLYWCH1/β-catenin interaction, we first carried out a coupled *in-vitro* transcription/translation (IVT) assay of both FLYWCH1 and β-catenin in the presence and absence of constitutively active GSK-3β. Treatment of the IVT product with λ-phosphatase resulted in a single un-phosphorylated, faster-migrating form of FLAG-β-catenin^{WT} resembling FLAG-β-catenin^{S33A} (Fig S1B, bottom panel, lanes 2 and 3). Interestingly, our IP assay (using α-GFP antibody) confirmed the interaction of GFP-FLYWCH1 with both FLAG-β-catenin^{WT} (treated with λ-phosphatase) and FLAG-β-catenin^{S33A} (Fig S1B, top panel, lanes 2 and 3).

Next, to further address the association of un-phosphorylated β-catenin with FLYWCH1, we expressed and purified GST-β-catenin^{WT}, GST-β-catenin^{4A} and His-FLYWCH1 proteins from bacteria for an *in vitro* binding assay. Co-immunoprecipitation (Co-IP) with His-antibody and WB with β-catenin-antibody revealed that FLYWCH1 could directly bind the un-phosphorylated β-catenin^{4A} (a mutant clone that lacks the phosphorylation sites S33, S37, and S45 which needed to prime β-catenin for subsequent phosphorylation at S41, S33, and S37 by GSK-3) (Fig 1F). We also confirmed the interaction of GFP-FLYWCH1 with ectopically expressed β-catenin (FLAG-β-catenin^{S33A} and FLAG-β-catenin^{4A}) in HEK293 cells using both α-GFP and α-FLAG antibodies respectively (Figs 1G and S1C). Further Co-IP analyses showed that β-catenin^{4A} interacts with FLYWCH1

regardless of GSK status (Fig S1D, lane 3 vs lane 4). A single mutation of β-catenin (β-catenin^{S33A}) showed stronger interaction with FLYWCH1 than the wild-type (β-catenin^{WT}) (Fig S1D, lane 5 vs lane 1), whereas the GSK3 inhibitor-BIO enhanced the interaction of both β-catenin^{S33A} and β-catenin^{WT} with FLYWCH1 (Fig S1D, lanes 6 and 2). Overall, these data indicate that phosphorylation of any of these sites may dampen the FLYWCH1 interaction with β-catenin.

The β-catenin has three main domains, the N-terminus, C-terminus and the armadillo repeats, to which most of its nuclear partners bind (27-29). Thus, we generated a series of β-catenin internal deletions to investigate which region is involved in the FLYWCH1/β-catenin interaction (Fig S2A). Two β-catenin mutants (MD3 and ΔC) were weakly expressed, presumably due to their degradation in the cytoplasmic β-catenin-destruction complexes (Fig S2A, lanes 7 and 8). These two deletions were therefore excluded from further Co-IP analyses. Co-IP analysis showed that the N-terminal deletion of β-catenin (ΔN) was sufficient to abort FLYWCH1/β-catenin interaction (Fig 1H). The β-catenin protein has no classical nuclear-localisation or nuclear export signals (30). Therefore, β-catenin deletions may not affect the subcellular distribution of the mutant proteins. Intriguingly, the armadillo repeats region of β-catenin (represented by deletions MD1 and MD2 in Fig S2A) containing the TCF/LEF binding domain was not essential for this interaction (Fig 1H). Furthermore, we generated several deletion mutant clones of FLYWCH1 to map the interaction of FLYWCH1 with β-catenin, (Figs S2, B-D). Co-IP revealed that β-catenin lost its interaction with the C-terminal deletion mutant of FLYWCH1 (ΔC350) in which the last two FLYWCH motifs are removed (Fig S2E). Full-length FLYWCH1 is expressed in the nucleus in a punctate format (Fig S3A) presumably due to the presence of an NLS within the C-terminus domain (Fig S1A). However, the protein product of GFP-FLYWCH1-ΔC350 is diffused into both the

cytoplasm and nucleus (Fig S3A), and a significant fraction of its protein remained in the nucleus (Fig S3B). Therefore, the cellular distribution of FLYWCH1-ΔC350 protein may not result in a complete loss of FLYWCH1/β-catenin interaction. Next, we investigated the interaction of FLYWCH1 with endogenous β-catenin in SW480 cells which contain a high level of nuclear β-catenin due to mutations in the APC gene. Our Co-IP assay showed a direct interaction between endogenous β-catenin and FLYWCH1, while the C-terminal deletion of FLYWCH1 (ΔC350) has lost the ability to interact (Fig 1I). Taken together these data suggest that the FLYWCH1-C-terminus domain is essential for efficient β-catenin interaction and complete nuclear-localisation of FLYWCH1.

FLYWCH1 represses the transcriptional activity of β-catenin by preventing the association of TCF4/β-catenin to the *Tcf*-DNA-binding elements

To elucidate the consequences of FLYWCH1/β-catenin interaction on the transcriptional activity of β-catenin/TCF4, we first performed a dual-luciferase TOP/FOP-FLASH reporter assay as described previously (20, 21). Intriguingly, FLYWCH1 effectively suppressed the reporter activity induced by β-catenin in different cell lines (Figs 2A and S3C). The luciferase-activity of all deletion mutants of β-catenin except the N-terminal deletion (β-catenin−ΔN) was significantly inhibited by FLYWCH1 (Fig S3D, lane3). Similarly, the C-terminus removal of FLYWCH1 (ΔC350) has lost its suppressive activity against β-catenin signalling (Fig 2B, lane 6). Thus, in line with our Co-IP results, the luciferase data also confirmed that the β-catenin-N-terminus and the FLYWCH1-C-terminus are required for both their physical and functional interaction.

To explore the downstream effect of the functional interaction of FLYWCH1/β-catenin, we show that the *c-jun*-promoter-Luc (a putative β-catenin-target gene) was effectively

suppressed by FLYWCH1 (Fig 2C). This suppression, however, was impaired by *FLYWCH1*-siRNA, while the TCF4 and β-catenin protein levels were unaffected (Fig 2C). Intriguingly, our Co-IP assays showed that the interaction between β-catenin and TCF4 is mitigated by the ectopic expression of FLYWCH1 (Fig 2D). Moreover, the luciferase assay showed that overexpression of TCF4 only slightly rescued the suppression effect of FLYWCH1 on β-catenin (Fig 2E) giving the notion that FLYWCH1 may compete with TCF4 for binding to β-catenin. To further confirm this notion, we performed a competitive binding assay of human β-catenin protein to determine if the β-catenin and TCF4 interaction values influenced by FLYWCH1 using competition and an ELISA based binding assays *in vitro* (Fig S4, A-C). The result shows that FLYWCH1 protein, indeed, competes with TCF4 protein for binding to β-catenin.

FLYWCH1 may compete with TCF4 via its binding to the *Tcf*-DNA binding sites. To explore this possibility, we first employed the LightShift Chemiluminescent EMSA assay using SW480 nuclear protein extract incubated with a biotin end-labelled DNA contains 3x of *Tcf*-DNA-binding site in the absent and/or present of recombinant TCF4 and FLYWCH1 proteins. Interestingly, the amount of DNA-TCF4-protein interaction is substantially reduced by FLYWCH1 protein (Fig S4D). Our biotinylated-oligonucleotide-mediated chromatin-immunoprecipitation (ChIP) assay (31) also showed that the biotinylated oligos (containing x3 *Tcf*-DNA consensus sites, TOP) could not equally pull-down the HA-TCF4 from streptavidin/biotinylated beads in the presence of MYC-FLYWCH1 (Fig 2F). Furthermore, our endogenous TCF4-ChIP assay in HCT116 cells (contains high endogenous level of TCF4) show that binding of the TCF4 to the *Tcf*-sites of the *c-jun*-promoter was reduced by both endogenous and exogenous levels of FLYWCH1 (Fig 2G). These data strongly indicate the competition of FLYWCH1 with TCF4 to bind to the *Tcf*-DNA binding sites.

Next, we assessed the role of β-catenin in this competition. Our data show that knockdown of β-catenin (20) remarkably rescued the suppression effect of FLYWCH1 (Fig 2H), indicating the necessity of β-catenin for the FLYWCH1-mediated transcriptional repression. To further support this notion, we performed a β-catenin-ChIP assay based on standard and qPCR analysis (Fig 3, A-B) to the *Tcf*-DNA-binding sites within *c-jun* promoter. β-catenin-ChIP experiments were performed in normal fibroblasts (TIG119) that lack nuclear-β-catenin (Fig S4E) (21) and CRC cells (DLD-1 and SW480) that contain nuclear β-catenin. Notably, in contrast to the TIG119 cells, immunofluorescent assay demonstrated that the β-catenin differentially expressed in the normal colonic epithelial cell line CCD-CoN-841, including some nuclear expression (Fig S4E). Expectedly, the ChIP assays showed an efficient binding of both β-catenin/TCF4 and β-catenin/FLYWCH1 (to a different extent) to the *Tcf*-DNA-binding elements of the *c-jun*-promoter in CRC cells, but not fibroblasts (Fig 3A). These data further confirm the β-catenin dependency of the FLYWCH1-mediated transcriptional repression. Moreover, FLYWCH1 overexpression also reduced the interaction of β-catenin/TCF4 to the *c-jun-Tcf*-sites (Fig 3B). We also show that the competition of FLYWCH1 and TCF4 to the *Tcf*-DNA-binding elements, is not through the direct interaction of TCF4 and FLYWCH1 proteins as no FLYWCH1 was co-IPed with TCF4 in TIG119-fibroblasts that lack nuclear β-catenin (Fig S4F).

To elucidate the physiological relevance of FLYWCH1/β-catenin interaction and activation of Wnt-signaling, we examined the FLYWCH1 expression under the influence of canonical Wnt3a-ligand and R-spondin-1 that bind to and activate Wnt-receptors (32, 33). The WB assays showed that Wnt3a/R-Spondin treatment remarkably increased the accumulation of nuclear β-catenin and Wnt-target genes such as cyclin-D1 and c-Jun (Fig 3C), while downregulated the *FLYWCH*1 gene expression (Fig 3, D-E). Further analyses

showed that overexpression of FLYWCH1 in the Wnt3a/R-Spondin-treated SW480 cells leads to decreased expression of both cyclin-D1 and cyclin-D2 (Fig 3F, lane 3 vs lane 4), indicating that FLYWCH1 acts as a negative transcriptional modulator for the Wnt-target genes.

Altogether, our findings suggest that FLYWCH1 represses the transcriptional activity of β-catenin by preventing the association of TCF4/β-catenin to the *Tcf*-DNA-binding elements via competing with TCF4. Our data also indicate that FLYWCH1 may act as a negative regulator of Wnt/β-catenin signalling pathway through transcriptional repression of Wnt-target genes.

FLYWCH1 modulates cell morphology

To explore the biological activity of FLYWCH1, we first examined FLYWCH1 transfected cells under the microscope and observed changes in cell shape and morphology. It is noteworthy to mention that stable overexpression of full-length FLYWCH1 has been attempted in SW480 and HCT116 cells using GFP-FLYWCH1 lentiviral vector (*p*LVX-GFP-FLYWCH1-Puro^{R}) based on Puro-selection with no success (Fig S5A). GFP-FLYWCH1 showed different cellular localisation pattern (Fig S5A) and different truncated forms of the protein (Fig S5B) indicating possible spontaneous mutation(s) of FLYWCH1 in these cell lines. To explore this possibility, the N-terminal coding region of the genome-integrated FLYWCH1 flanked by eGFP was amplified by PCR and sequenced. Expectedly, the sequencing analysis revealed a point mutation, resulted in a stop-codon at aa277 (stable ≠1), and a relatively large internal in-frame deletion (537nt) mapped to nucleotides 1405-1942 within the C-terminal domain (Δ468-648aa, stable ≠2) of FLYWCH1 (Fig S5, C-D). These deletions were corresponding to the truncated protein bands detected on WB (Fig S5B).

Indeed, consistent with our previous data, the stably expressed truncated form of FLYWCH1 (Δ468-648aa) lost its physical interaction and suppression activity against TCF4/β-catenin (Fig S5, E-F). Data from the COSMIC (The catalogue of Somatic Mutations in Cancer) database revealed that somatic mutation in FLYWCH1 is rare in human cancers. Out of 32,801 primary human cancer samples, only 154 samples (a mutation rate of 0.47%) have somatic mutations. Interestingly, over 23% of these mutations found in the large intestine and 3.9% of these were frameshift deletions (Fig S6A). Therefore, CRC cells transiently expressing GFP-FLYWCH1 were used for biological analysis.

With the possible frameshift mutation and loss of action associated with FLYWCH1 overexpressing cells, we first, tested the effect of FLYWCH1-knockdown on cell cycle progression in SW480 and HCT116 cells stained with Propidium iodide (PI) using flow cytometric analyses. We observed that FLYWCH1-knockdown increased cell number at G2/M transition in both SW40 and HCT116 cells (Fig S6B). Next, we tested the morphological changes associated to transient overexpression of FLYWCH1. Our microscopic study for Phalloidin stained SW480 cells showed that untransfected cells displayed branched, flat, and elongated shape with prominent actin fibres. While, FLYWCH1-expressing cells showed a different phenotype, characterised by shorter, circular epithelial-like morphology with actin fibres concentrated at the edges of the cells (Figs 4A, middle horizontal panel). Consistent with this observation, *FLYWCH*1-knockdown cells exhibited irregular branched shapes with numerous elongated projections (filopodia) in all directions compared to controls (Fig 4A, lower panel and Fig S7, C-D and F vs G), suggesting that FLYWCH1 may modulate cellular biological activities through changes in cell morphology.

Previous studies have showed that β-catenin protein complexes redistribute from the membrane to the nucleus upon Wnt, Irradiation, TGF-β1, and Rac1 activation or fibrosis and the nuclear substructures formed were readily identifiable (34-38). To explore this, we tested TIG119 cells, a normal embryonic fibroblast lacking nuclear β-catenin (Fig S4E), when treated with Wnt3A and stained for anti-β-catenin (Fig S7I). Thus, activation of β-catenin signaling may show a nuclear substructures foci-like pattern similar to the sub-nuclear localization of FLYWCH1.

Changes in cell morphology through actin cytoskeleton reorganisation and filopodia formation have been involved in cell proliferation, migration and invasion (39, 40). Therefore, we investigated whether alteration of cell morphology caused by FLYWCH1 correlates to cell motility. Interestingly, our *in-vitro* scratch assay showed that the wound-closure of FLYWCH1 expressing cells versus *FLYWCH*1-knockdown and control cells is significantly reduced in SW480 cells (Figs 4B and S7E), indicating negative effect of FLYWCH1 on cell migration. To further delineate the effect of FLYWCH1 on cell attachment and motility, we evaluated the attachment and spreading capacity of FACS-sorted SW480-expressing GFP, GFP-FLYWCH1, and GFP-FLYWCH1^{shRNA} using electric cell-substrate impedance sensing (ECIS) (41). The ECIS analyses showed that cells overexpressing GFP-FLYWCH1 established a significantly higher resistance value comparing to FLYWCH1^{shRNA} and control cells (~6000 ohms vs 2000- ~3000ohm). But the capacitance decreases in cells overexpressing GFP-FLYWCH1 versus *FLYWCH1*-knockdown and control cells (~1.5F vs ~2.5- ~4μF) (Fig 4C, right panel). These data indicate migration/invasion defects caused by FLYWCH1 possibly due to increased cell-cell attachment. Indeed, the ECIS analyses showed that cells-expressing GFP-FLYWCH1 were quickly and tightly attached within 1-2hrs period compared to cells-expressing GFP (10-12hrs), whereas cells-expressing FLYWCH1^{shRNA}

were delayed for over 24hrs (Fig 4C, left panel). Also, cells-expressing GFP-FLYWCH1 have restricted the current flow by slow spreading over the electrode leading linearly to decreased capacitance. This indicates increased cell attachment of GFP-FLYWCH1 overexpressing cells. To investigate if such activity may also modulate metastatic CRC cells, we tested the effects of FLYWCH1 on cell morphology and migration using a metastatic CRC cell line, SW620 (Fig S8, A-C). These data indicate that FLYWCH1 inhibits cell migration and invasion in SW620 cells. Thus, these results suggest that FLYWCH1 may negatively regulate cell migration through alterations in cell-cell adhesion.

Molecular mechanisms of FLYWCH1-regulated cell migration

To explore the mechanisms underlying the effect of FLYWCH1 on cell migration, we first used a human WNT-signalling pathway cDNA-array to determine the expression profiles of 84 genes related to WNT-mediated signal transduction according to the manufacturer's instructions; http://www.sabiosciences.com/rt_pcr_product/HTML/PAHS-243Z.html (Table S2). These data further highlighted differences in transcript expression between FACS-sorted cells overexpressing GFP-FLYWCH1 and GFP proteins. Notably, many of these changes associated with cell polarity and invasion (e.g., MMP7, DVL, FZD, JUN, and several WNT-target genes) (Fig 5A and Table S2). Interestingly, our further qRT-PCR analysis showed that expression of a limited subset of genes (*CD*44, *LGR*5, *c-JUN*, *EPHA*4, *CCND*1, *EFNB*2 and *FSCN*1) were suppressed by the ectopic expression of FLYWCH1, while expression of others (*c-MYC*, *EFNB*1, *EPHB*2 and *EPHB*3) were unaffected in both SW480 and HCT116 cells (Fig 5B, left panel, blue columns). Strikingly, the transcriptional repression of *CD*44, *LGR*5, *c-JUN*, *EPHA*4, *CCND*1, *EFNB*2, *FSCN*1, *ZEB*1, and c-*MYC* was significantly reversed by the *FLYWCH*1-knockdown, while the expression of others such as *EFNB*1 and *EPHB*3 were unchanged (Fig 5B, left panel, red columns). These data suggest selective repression of Wnt-

target genes via FLYWCH1/β-catenin interaction. Moreover, our WB analysis showed a sufficient correlation between transcript and protein levels of some of these target genes in FLYWCH1-knockdown cells but less correlation in FLYWCH1-overexpressing cells (Fig 5B, right panel). Not surprising that mRNA levels cannot always correspond to protein levels due to posttranslational modifications (42). Furthermore, in a normal embryonic fibroblast lacking nuclear β-catenin and stably expressing the MYC-FLYWCH1, the cyclin-D1 expression is downregulated whereas *FSCN*1, *SFRP1*, *c-MYC* and the *c-JUN* mRNA levels remained unchanged (Fig S8, D-E) further supporting the notion of selective negative regulation of Wnt-target genes by FLYWCH1/β-catenin interaction. However, effects of FLYWCH1 on cyclin-D1 gene expression via β-catenin-independent TCF/LEF activity cannot be excluded.

Notably, the expression of the cell-cell adhesion receptor, E-cadherin (*CDH*1) was upregulated by FLYWCH1 overexpression in contrast to *FLYWCH1*-knockdown. Some of the pre-mentioned responded genes such as *ZEB*1, *CDH*1, and *EPHA*4 are well known for their involvement in epithelial-mesenchymal transition (EMT) and cell migration. Thus, next, we asked if FLYWCH1 could regulate cell migration via EMT/MET process. Our WB showed no significant differences in the levels of a mesenchymal marker, Vimentin or an EMT transcription factor, ZEB2 (Fig 5C). However, significant differences between E-cadherin and ZEB1 mRNA and protein expression were detected in response to the presence and/or absence of FLYWCH1 (see above and Fig 5, B-C). Moreover, the level of Snail protein is accumulated in FLYWCH-knocked down cells (similar to ZEB1), while the level of Twist protein is downregulated (Fig S9A). Overall, these data suggest a synergistic action of these EMT-activating transcription factors may ultimately lead to a partial or steady state level of EMT process transition in CRC cells with altered FLYWCH1 expression. However, further investigation is required to explore the possible mechanism in more details.

Previous studies found that β-catenin/TCF4 activity modulates expression of *ZEB*1 in SW480 cells (43). Accordingly, it is expected that FLYWCH1 interaction with β-catenin may also regulate β-catenin-mediated transcription of ZEB1. Indeed, overexpression of FLYWCH1 massively decreased the transcription of human *ZEB*1-promoter in SW480 cells (Fig 5, D-E). This effect, however, was not found when a mutant form of FLYWCH1 (FLYWCH1ΔC) which lacks the β-catenin-binding domain was used (Fig 5D). Notably, overexpression of ZEB1 rescued the inhibitory effect of FLYWCH1 overexpression on cell migration (Fig S9, B-C). These data support the notion that FLYWCH1-mediated suppression of *ZEB*1 may depend on the formation of a transcriptional activation complex with nuclear β-catenin.

*ZEB*1 and *EPHA*4 which were among the most affected genes by the *FLYWCH1*-knockdown (Fig 5B) are important determinants of tumour progression serving as an inducer of invasion and metastasis in CRCs (44, 45). Therefore, we sought to examine whether the expression of *FLYWCH*1 correlates with the expressions of these genes in human pathological samples. First, to examine the correlation between FLYWCH1 and ZEB1, CDH1 and EPHA4 gene expression, we obtained the expression data of colon cancer from the TCGA. Level 3 Illumina RNA-Seq data for colon adenocarcinoma (COAD) were downloaded from cBioPortal, which contained gene expression data for 469 primary tumour samples of COAD (Fig S9, D-G). The data indicated a significant negative correlation between FLYWCH1 and ZEB1 and EPHA4 (Fig S9D and S9E), whereas the correlation between FLYWCH1 and CDH1 or ZEB1 and CDH1 is very weak and is not significant (Fig S9F and S9G). These data suggest that FLYWCH1 may possess some anti-metastatic activity.

Next, the expression of *FLYWCH*1 in a series of early and advanced/metastatic patient's CRCs was assessed using *in-situ* hybridization (ISH) assay on a tissue microarray

(TMA). Our analysis showed a negative correlation between *FLYWCH*1 expression and tumour progression (70.8% vs. 25.7%, p≤0.017, Fig 6A). Furthermore, the expression pattern of *ZEB*1 and *EPHA*4 versus *FLYWCH*1 in a cohort of 33 (normal, primary and metastatic) tumour tissues were also investigated. Our data showed that *ZEB*1 expression is highly increased in advanced tumours, while *FLYWCH*1 expression is significantly repressed (Fig 6B). Interestingly, a significant linear correlation between down-regulation of *FLYWCH*1 and upregulation of *ZEB*1 and *EPHA*4 in normal versus advanced stages, but not in the primary tumours, was observed (Fig 6B).

Discussion

Despite the fact that substantial progress toward identification of full human proteome, not all the annotated protein-coding genes have been characterized. One such example is the protein product of *FLYWCH*1 gene which contains five conserved FLYWCH-type Zinc-finger domains (Fig. 1). This work demonstrates identification, characterization and functional analysis of FLYWCH1 protein for the first time. Based on bioinformatics analysis, FLYWCH1 may have potential DNA-binding abilities due to the presence of highly conserved NLS and FLYWCH-type Zinc-finger motifs which appears to be evolutionarily conserved in mammals (Figs 1 and S1). It should be noted that, although the endogenous FLYWCH1 can be detected by IF, despite lot of efforts no commercial antibody can detect the endogenous FLYWCH1 by WB or immunohistochemistry analysis.

We demonstrated that FLYWCH1 inhibits β-catenin-mediated transcriptional activation by competing with TCF4 to bind to β-catenin. We also show direct evidence of cell migration and invasion defects caused by overexpression of FLYWCH1 that mimic a

canonical Wnt loss-of-function phenotype. Moreover, our analyses revealed repression of a surprisingly limited sub-set of β-catenin-target genes by FLYWCH1 including those involved in regulation of cell migration and morphology. Alterations in cell motility and morphology are initial steps toward invasion and metastasis, one of the critical hallmark of cancer. Wnt/β-catenin signalling pathway, through different mechanisms, is often linked to regulation of various biological traits such as modulation of collective cell migration and cell branching (46-48). Indeed, signalling through this pathway modulates the expression of multiple genes that control filopodia formation and consequently, cell morphology, migration, and invasion. Examples of these genes include CDH1, Fascin1, c-Jun, and Eph/ephrin molecules (49-52). One of the most widely studied critical protein for the establishment of filopodia is the actin-binding protein, Fascin. Notably, our data show that Fascin1 gene expression is regulated by FLYWCH1 (Fig 5B). During development, Fascin promotes cell migration through filopodia formation. High Fascin expression is correlated with invasion and metastasis of various tumours (53, 54).

In line with these findings, the reduced cell migration and morphological changes observed in this study might be due to modulation of the genetic program downstream of β-catenin/TCF4 by FLYWCH1. Especially, as FLYWCH1 negatively regulates the β-catenin/TCF transactivation with no effect on the level of either β-catenin or TCF4 proteins (Fig 2). The possible mechanism by which continuous Wnt3a/R-spondin1 treatment downregulates *FLYWCH*1 is currently unclear. It is possible that the Wnt/β-catenin-TCF4 via a negative feedback loop regulates the FLYWCH1 transcription product. In turn, FLYWCH1, together with Wnt via the β-catenin/TCF4, activates “on” or “off” decision to control the downstream genes fundamental to cell migration. Although this genetic modulation is likely to represent a transcriptional hierarchy, nevertheless, it is essential to understand why and

how FLYWCH1 selectively represses specific β-catenin/TCF-target genes and uncover the molecular mechanisms behind this. The current study, so far, focused on the assessment of the consequences of FLYWCH1 aberrations on the Wnt/β-catenin canonical pathway. However, a possible role of FLYWCH1 in combination with different ligands and receptors in regulating cell morphology and migration via alternative non-canonical Wnt/signalling responses (for example, mediated by small GTPases, Rac1 and RhoA) (55), remains unknown.

Defects in cell migration and actin cytoskeleton rearrangement could be related to EMT (56). However, the decreased cell migration found in our study is likely due to mechanisms other than EMT. No significant change in Vimentin expression indicates that its expression might not be regulated by FLYWCH1 and, thereby, ruling out the involvement of FLYWCH1 during EMT. Thus, it appears that FLYWCH1 may control cell migration via β-catenin-dependent E-cadherin upregulation and ZEB1 downregulation leading to increased cell-cell and cell-matrix adhesion.

The role of E-cadherin and the adherens junctions in mediating epithelial differentiation, by the establishment of cellular adhesion and polarity, is well recognised. Consistent with our observations, upregulation of E-cadherin has been widely associated with reduced cell motility and invasion in addition to morphological changes from mesenchymal-like to epithelial-like shape in various types of cancer (57, 58). Another interesting observation of our study is the negative correlation between *FLYWCH*1 expression and tumour progression (Fig 6, A-B). One possible hypothesis is that tumour cells have developed mechanisms to suppress FLYWCH1 expression (Fig 6C), facilitating changes in cell morphology and migration which promotes metastasis. FLYWCH1 is a newly characterised gene. Our findings demonstrate that FLYWCH1 could have potential tumour suppressor

activity. In advanced CRC, FLYWCH1 similar to most tumour suppressor genes is significantly inhibited. A likely hypothesis is that tumours with high degrees of methylation are more likely to inactivate genes critical for tumour progression and metastasis. However, the underlying mechanisms associated with the possible epigenetic and posttranscriptional regulation of FLYWCH1 gene expression remained unknown. Furthermore, FLYWCH1 functions as a transcription modulator that can bind to DNA and/or RNA and in β-catenin-dependent or independent manners. Therefore, outside the scope of the current studies, a comprehensive genomic analysis to identify the direct target genes regulated by FLYWCH1, using both ChIP-sequencing and RNA-sequencing or RIP-sequencing analyses, will further clarify other functions of this protein.

In conclusion, our findings revealed a new molecular mechanism underlying negative signal cross-talk between FLYWCH1 and β-catenin. In this manner, the FLYWCH1/β-catenin complex represses selective Wnt-target genes, including *Eph/ephrin* and *ZEB*1, which mainly associated with cell polarity and migration during CRC development and metastasis. Prospectively, FLYWCH1 has potential to represent a biomarker and therapeutic target against metastatic CRC in the future.

Supplementary Information

Supplementary Information includes; 9 Figures, and 2 Tables can be found with this article online at *Molecular Cancer Research* website.

Acknowledgements

We are grateful to B.W. O'Malley, M. Saito and A. McIntyre for providing essential reagents. We thank R. Muraleedharan and W. Fadhil for technical help and advice on histology. We

also thank the fantastic fundraising efforts of Alison Sims and her family in memory of Daz Sims to support the work in our laboratory. This work was supported by the Medical Research Council research grant G0700763 to A.S.N. and University of Nottingham, UK.

Author Contributions

B.A.M., S.A., E.K.O, A.S., S.H.K., A.L., and R.B-J are contributed to acquisition of data, and/or analysis, interpretation of data and drafting the article. B.S-D contributed to acquisition of data and reviewing the article critically, and M.I and A.B provision of study material and reviewing the article critically. A.S.N participated in study conception, design and supervision, obtained funding, drafting the article and revising it critically.

References

1. Akiyama H, Lyons JP, Mori-Akiyama Y, Yang X, Zhang R, Zhang Z, et al. Interactions between Sox9 and beta-catenin control chondrocyte differentiation. Genes & development. 2004;18(9):1072-87.

2. Ito K, Lim AC, Salto-Tellez M, Motoda L, Osato M, Chuang LS, et al. RUNX3 attenuates beta-catenin/T cell factors in intestinal tumorigenesis. Cancer Cell. 2008;14(3):226-37.

3. Takemaru K, Yamaguchi S, Lee YS, Zhang Y, Carthew RW, Moon RT. Chibby, a nuclear beta-catenin-associated antagonist of the Wnt/Wingless pathway. Nature. 2003;422(6934):905-9.

4. Olson LE, Tollkuhn J, Scafoglio C, Krones A, Zhang J, Ohgi KA, et al. Homeodomain-mediated beta-catenin-dependent switching events dictate cell-lineage determination. Cell. 2006;125(3):593-605.

5. Kelly KF, Ng DY, Jayakumaran G, Wood GA, Koide H, Doble BW. beta-catenin enhances Oct-4 activity and reinforces pluripotency through a TCF-independent mechanism. Cell Stem Cell. 2011;8(2):214-27.

6. Barker N, Hurlstone A, Musisi H, Miles A, Bienz M, Clevers H. The chromatin remodelling factor Brg-1 interacts with beta-catenin to promote target gene activation. EMBO J. 2001;20(17):4935-43.

7. Hecht A, Vleminckx K, Stemmler MP, van Roy F, Kemler R. The p300/CBP acetyltransferases function as transcriptional coactivators of beta-catenin in vertebrates. EMBO J. 2000;19(8):1839-50.

8. Townsley FM, Cliffe A, Bienz M. Pygopus and Legless target Armadillo/beta-catenin to the nucleus to enable its transcriptional co-activator function. Nat Cell Biol. 2004;6(7):626-33.

9. Wu Y, Zhang Y, Zhang H, Yang X, Wang Y, Ren F, et al. p15RS attenuates Wnt/{beta}-catenin signaling by disrupting {beta}-catenin.TCF4 Interaction. J Biol Chem. 2010;285(45):34621-31.

10. Easwaran V, Pishvaian M, Salimuddin, Byers S. Cross-regulation of beta-catenin-LEF/TCF and retinoid signaling pathways. Curr Biol. 1999;9(23):1415-8.

11. Kaidi A, Williams AC, Paraskeva C. Interaction between beta-catenin and HIF-1 promotes cellular adaptation to hypoxia. Nat Cell Biol. 2007;9(2):210-7.

12. Evans PM, Chen X, Zhang W, Liu C. KLF4 interacts with beta-catenin/TCF4 and blocks p300/CBP recruitment by beta-catenin. Mol Cell Biol. 2010;30(2):372-81.

13. Ulloa F, Itasaki N, Briscoe J. Inhibitory Gli3 activity negatively regulates Wnt/beta-catenin signaling. Curr Biol. 2007;17(6):545-50.

14. Valenta T, Lukas J, Doubravska L, Fafilek B, Korinek V. HIC1 attenuates Wnt signaling by recruitment of TCF-4 and beta-catenin to the nuclear bodies. EMBO J. 2006;25(11):2326-37.

15. Zhang W, Chen X, Kato Y, Evans PM, Yuan S, Yang J, et al. Novel cross talk of Kruppel-like factor 4 and beta-catenin regulates normal intestinal homeostasis and tumor repression. Mol Cell Biol. 2006;26(6):2055-64.

16. Dai MS, Sun XX, Qin J, Smolik SM, Lu H. Identification and characterization of a novel Drosophila melanogaster glutathione S-transferase-containing FLYWCH zinc finger protein. Gene. 2004;342(1):49-56.

17. Dorn R, Krauss V. The modifier of mdg4 locus in Drosophila: functional complexity is resolved by trans splicing. Genetica. 2003;117(2-3):165-77.

18. Beaster-Jones L, Okkema PG. DNA binding and in vivo function of C.elegans PEB-1 require a conserved FLYWCH motif. Journal of molecular biology. 2004;339(4):695-706.

19. Ow MC, Martinez NJ, Olsen PH, Silverman HS, Barrasa MI, Conradt B, et al. The FLYWCH transcription factors FLH-1, FLH-2, and FLH-3 repress embryonic expression of microRNA genes in C. elegans. Genes Dev. 2008;22(18):2520-34.

20. Ibrahim EE, Babaei-Jadidi R, Saadeddin A, Spencer-Dene B, Hossaini S, Abuzinadah M, et al. Embryonic NANOG activity defines colorectal cancer stem cells and modulates through AP1- and TCF-dependent mechanisms. Stem cells (Dayton, Ohio). 2012;30(10):2076-87.

21. Nateri AS, Spencer-Dene B, Behrens A. Interaction of phosphorylated c-Jun with TCF4 regulates intestinal cancer development. Nature. 2005;437(7056):281-5.

22. Park CY, Kim HS, Jang J, Lee H, Lee JS, Yoo JE, et al. ABCD2 is a direct target of beta-catenin and TCF-4: implications for X-linked adrenoleukodystrophy therapy. PloS one. 2013;8(2):e56242.

23. Nateri AS, Riera-Sans L, Da Costa C, Behrens A. The ubiquitin ligase SCFFbw7 antagonizes apoptotic JNK signaling. Science. 2004;303(5662):1374-8.

24. Babaei-Jadidi R, Li N, Saadeddin A, Spencer-Dene B, Jandke A, Muhammad B, et al. FBXW7 influences murine intestinal homeostasis and cancer, targeting Notch, Jun, and DEK for degradation. J Exp Med. 2011;208(2):295-312.

25. Lorenzi F, Babaei-Jadidi R, Sheard J, Spencer-Dene B, Nateri AS. Fbxw7-associated drug resistance is reversed by induction of terminal differentiation in murine intestinal organoid culture. Molecular Therapy — Methods & Clinical Development. 2016;3:16024.

26. Li N, Lorenzi F, Kalakouti E, Normatova M, Babaei-Jadidi R, Tomlinson I, et al. FBXW7-mutated colorectal cancer cells exhibit aberrant expression of phosphorylated-p53 at serine-15. Oncotarget. 2015.

27. Behrens J, von Kries JP, Kuhl M, Bruhn L, Wedlich D, Grosschedl R, et al. Functional interaction of beta-catenin with the transcription factor LEF-1. Nature. 1996;382(6592):638-42.

28. Graham TA, Weaver C, Mao F, Kimelman D, Xu W. Crystal structure of a beta-catenin/Tcf complex. Cell. 2000;103(6):885-96.

29. van de Wetering M, Cavallo R, Dooijes D, van Beest M, van Es J, Loureiro J, et al. Armadillo coactivates transcription driven by the product of the Drosophila segment polarity gene dTCF. Cell. 1997;88(6):789-99.

30. Huber AH, Weis WI. The structure of the beta-catenin/E-cadherin complex and the molecular basis of diverse ligand recognition by beta-catenin. Cell. 2001;105(3):391-402.

31. Kim J, Cantor AB, Orkin SH, Wang J. Use of in vivo biotinylation to study protein-protein and protein-DNA interactions in mouse embryonic stem cells. Nature protocols. 2009;4(4):506-17.

32. Nam JS, Turcotte TJ, Smith PF, Choi S, Yoon JK. Mouse cristin/R-spondin family proteins are novel ligands for the Frizzled 8 and LRP6 receptors and activate beta-catenin-dependent gene expression. J Biol Chem. 2006;281(19):13247-57.

33. Yamamoto H, Sakane H, Yamamoto H, Michiue T, Kikuchi A. Wnt3a and Dkk1 regulate distinct internalization pathways of LRP6 to tune the activation of beta-catenin signaling. Developmental cell. 2008;15(1):37-48.

34. Jamieson C, Lui C, Brocardo MG, Martino-Echarri E, Henderson BR. Rac1 augments Wnt signaling by stimulating beta-catenin-lymphoid enhancer factor-1 complex assembly independent of beta-catenin nuclear import. Journal of cell science. 2015;128(21):3933-46.

35. Conde-Perez A, Gros G, Longvert C, Pedersen M, Petit V, Aktary Z, et al. A caveolin-dependent and PI3K/AKT-independent role of PTEN in beta-catenin transcriptional activity. Nature communications. 2015;6:8093.

36. Derksen PW, Tjin E, Meijer HP, Klok MD, MacGillavry HD, van Oers MH, et al. Illegitimate WNT signaling promotes proliferation of multiple myeloma cells. Proc Natl Acad Sci U S A. 2004;101(16):6122-7.

37. Chen JH, Chen WL, Sider KL, Yip CY, Simmons CA. beta-catenin mediates mechanically regulated, transforming growth factor-beta1-induced myofibroblast differentiation of aortic valve interstitial cells. Arteriosclerosis, thrombosis, and vascular biology. 2011;31(3):590-7.

38. Lam AP, Flozak AS, Russell S, Wei J, Jain M, Mutlu GM, et al. Nuclear beta-catenin is increased in systemic sclerosis pulmonary fibrosis and promotes lung fibroblast migration and proliferation. American journal of respiratory cell and molecular biology. 2011;45(5):915-22.

39. Li A, Dawson JC, Forero-Vargas M, Spence HJ, Yu X, Konig I, et al. The actin-bundling protein fascin stabilizes actin in invadopodia and potentiates protrusive invasion. Curr Biol. 2010;20(4):339-45.

40. Vignjevic D, Kojima S, Aratyn Y, Danciu O, Svitkina T, Borisy GG. Role of fascin in filopodial protrusion. J Cell Biol. 2006;174(6):863-75.

41. Wegener J, Keese CR, Giaever I. Electric cell-substrate impedance sensing (ECIS) as a noninvasive means to monitor the kinetics of cell spreading to artificial surfaces. Experimental cell research. 2000;259(1):158-66.

42. Maier T, Guell M, Serrano L. Correlation of mRNA and protein in complex biological samples. FEBS letters. 2009;583(24):3966-73.

43. Sanchez-Tillo E, de Barrios O, Siles L, Cuatrecasas M, Castells A, Postigo A. beta-catenin/TCF4 complex induces the epithelial-to-mesenchymal transition (EMT)-activator ZEB1 to regulate tumor invasiveness. Proc Natl Acad Sci U S A. 2011;108(48):19204-9.

44. de Marcondes PG, Bastos LG, de-Freitas-Junior JC, Rocha MR, Morgado-Diaz JA. EphA4-mediated signaling regulates the aggressive phenotype of irradiation survivor colorectal cancer cells. Tumour biology : the journal of the International Society for Oncodevelopmental Biology and Medicine. 2016;37(9):12411-22.

45. Spaderna S, Schmalhofer O, Wahlbuhl M, Dimmler A, Bauer K, Sultan A, et al. The transcriptional repressor ZEB1 promotes metastasis and loss of cell polarity in cancer. Cancer Res. 2008;68(2):537-44.

46. Aman A, Piotrowski T. Wnt/beta-catenin and Fgf signaling control collective cell migration by restricting chemokine receptor expression. Dev Cell. 2008;15(5):749-61.

47. Humtsoe JO, Liu M, Malik AB, Wary KK. Lipid phosphate phosphatase 3 stabilization of beta-catenin induces endothelial cell migration and formation of branching point structures. Mol Cell Biol. 2010;30(7):1593-606.

48. Matsuda Y, Schlange T, Oakeley EJ, Boulay A, Hynes NE. WNT signaling enhances breast cancer cell motility and blockade of the WNT pathway by sFRP1 suppresses MDA-MB-231 xenograft growth. Breast Cancer Res. 2009;11(3):R32.

49. Alt-Holland A, Shamis Y, Riley KN, DesRochers TM, Fusenig NE, Herman IM, et al. E-cadherin suppression directs cytoskeletal rearrangement and intraepithelial tumor cell migration in 3D human skin equivalents. J Invest Dermatol. 2008;128(10):2498-507.

50. Bochenek ML, Dickinson S, Astin JW, Adams RH, Nobes CD. Ephrin-B2 regulates endothelial cell morphology and motility independently of Eph-receptor binding. J Cell Sci. 2010;123(Pt 8):1235-46.

51. Cortina C, Palomo-Ponce S, Iglesias M, Fernandez-Masip JL, Vivancos A, Whissell G, et al. EphB-ephrin-B interactions suppress colorectal cancer progression by compartmentalizing tumor cells. Nat Genet. 2007;39(11):1376-83.

52. Pasquale EB. Eph receptors and ephrins in cancer: bidirectional signalling and beyond. Nat Rev Cancer. 2010;10(3):165-80.

53. Adams JC. Roles of fascin in cell adhesion and motility. Current opinion in cell biology. 2004;16(5):590-6.

54. Hashimoto Y, Skacel M, Adams JC. Roles of fascin in human carcinoma motility and signaling: prospects for a novel biomarker? The international journal of biochemistry & cell biology. 2005;37(9):1787-804.

55. Schlessinger K, Hall A, Tolwinski N. Wnt signaling pathways meet Rho GTPases. Genes & development. 2009;23(3):265-77.

56. Nelson CM, Khauv D, Bissell MJ, Radisky DC. Change in cell shape is required for matrix metalloproteinase-induced epithelial-mesenchymal transition of mammary epithelial cells. J Cell Biochem. 2008;105(1):25-33.

57. Kajiyama H, Kikkawa F, Khin E, Shibata K, Ino K, Mizutani S. Dipeptidyl peptidase IV overexpression induces up-regulation of E-cadherin and tissue inhibitors of matrix

metalloproteinases, resulting in decreased invasive potential in ovarian carcinoma cells. Cancer Res. 2003;63(9):2278-83.

58. Mao Q, Li Y, Zheng X, Yang K, Shen H, Qin J, et al. Up-regulation of E-cadherin by small activating RNA inhibits cell invasion and migration in 5637 human bladder cancer cells. Biochemical and biophysical research communications. 2008;375(4):566-70.

Figures Legends

Figure 1. Identification of FLYWCH1 as an interacting protein with unphosphorylated-β-catenin in yeast cells, *in-vitro* and *in-vivo*

A, Schematic representation of the modified yeast two-hybrid Ras Recruitment System (RRS) shows candidates interact with phosphorylated (left) and/or unphosphorylated (right) β-catenin (see detailed description in the text). GDP, guanosine diphosphate; MP, Met3 promoter; pA, polyA signal; P, phosphorylated amino acid. **B, C,** Ras, GSK-3β, FLAG and phospho-β-catenin protein expression in yeast. Phospho-β-catenin is induced by withdrawal of methionine **(C)**. **D,** Tandem repeats of five FLYWCH encoding domains across human FLYWCH1 protein. **E,** Alignment of FLYWCH domains sequence of human FLYWCH1 showing the core aa residues (F, L, Y, W, C and H) of FLYWCH consensus sequence highlighted in yellow. The starting and ending residue numbers given for each domain indicate the actual aa numbers within the FLYWCH1 protein sequence. Identical residues are indicated by asterisks (*) at the bottom line and the non-identical residues by colons (:). **F,** His-tag pull-down using purified GST-β-catenin^{WT}, GST-β-catenin^{4A} and 6xHis-FLYWCH1, followed by immunoblotting with anti-β-catenin and anti-His antibodies in the present of GSK-3β. **G,** Co-IP and immunoblotting of HEK293T cells co-transfected with the indicated constructs using anti-FLAG-conjugated agarose beads for Co-IP and anti-GFP and anti-FLAG antibodies for immunoblotting as indicated. **H,** Co-IP and immunoblotting of HEK293T cells co-transfected with the indicated constructs using anti-FLAG-conjugated agarose beads for

Co-IP and, anti-GFP and anti-FLAG antibodies for immunoblotting. In top panels, arrowhead indicates protein bands of GFP-FLYWCH1 detected by the anti-GFP antibody on both Co-IP and input membranes. In bottom panels, arrowheads indicate protein bands of FLAG-β-catenin, and mutants detected by anti-FLAG antibody on both IP and input membranes. Asterisks (*) indicate unspecific bands. **I,** Endogenous interaction between β-catenin and FLYWCH1 in the lysate of SW480 cells transfected with the indicated constructs. Co-IP was performed using anti-β-catenin-conjugated agarose beads. Normal IgG (IgG) was used as a negative control. The immunoprecipitated complexes were analyzed by WB with anti-β-catenin and anti-MYC antibodies. Asterisks (*) indicate unspecific bands.

Figure 2. FLYWCH1 competes with TCF4 for binding to β-catenin

A, Effect of overexpressed FLYWCH1 on the firefly luciferase reporter (TOP-FLASH) induced by the endogenous level of β-catenin in CRC cell-lines (SW480, HCT116 and SW620). Data are mean ± SD (n = 6; **, $P < 0.01$; ***, $P < 0.001$). **B,** FLYWCH1 C-terminal deletion (ΔC350) lost the ability to repress β-catenin^{S33A} activity (lane 6). Data are mean ± SD (n = 3; ***, $P < 0.001$). **C,** Suppression of the β-catenin^{S33A}-induced c-*jun* promoter activity by FLYWCH1. Data are mean ± SD (n = 6; **, $P < 0.01$; ***, $P < 0.001$). **D,** Co-IP of HEK293T lysate co-transfected with the indicated constructs using anti-FLAG-conjugated agarose beads. Both the Input and Co-IP samples were immunoblotted with anti-HA and anti-GFP antibodies. Asterisks (*) indicate unspecific bands. **E,** Effect of overexpressed FLYWCH1 on the firefly luciferase reporter (TOP-FLASH) induced by the overexpressed TCF4/β-catenin in HEK293T cells as indicated. Data are mean ± SD (n = 6; ***, $P < 0.001$). **F,** Schematic diagram of a biotinylated-oligonucleotide-mediated ChIP method shows the streptavidin/biotinylated *Tcf*/*Lef*-protein bound complex (upper panel) and immunoblots for

the indicated constructs using the anti-HA antibody for TCF4 (lower panels). The streptavidin/biotinylated DNA/protein-bound complexes were immunoprecipitated using streptavidin-coupled Dynabeads. Biotinylated oligos containing x3 *Tcf*-DNA consensus sites (TOP), could not equally pull-down the HA-TCF4 from streptavidin/biotinylated beads in the lysate of SW480 cells transfected with the MYC-FLYWCH1 or empty vector. The experiment was repeated on three independent occasions. **G,** Quantitative PCR analysis of *Tcf*-DNA-binding sites in the *c-jun* promoter to monitor chromatin occupancy of TCF4 by chromatin immunoprecipitation (ChIP) on sorted for GFP+ cells by flow-cytometry using HCT116 cells transfected with GFP-FLYWCH1, GFP and HA-TCF4 respectively. Data are mean ± SD (n = 3; *, $P < 0.05$; **, $P < 0.01$). **H,** Effect of shRNA-mediated knockdown of β-catenin, compared with the control scrambled control shRNA (scs) on the transcriptional repression of firefly luciferase reporter (TOP-FLASH) mediated by FLYWCH1 in SW480 cells. Data are mean ± SD (n = 6; ***, $P < 0.001$).

Figure 3. Competition between FLYWCH1/β-catenin and TCF4/β-catenin complexes for their interaction to *Tcf*-DNA-binding sites

A, β-catenin-ChIP assay shows binding of FLYWCH1/β-catenin and TCF4/β-catenin complexes to the human *c-jun* promoter in SW480 and DLD-1 cells (right panels), as well as TIG119 fibroblasts (left panel). SW480 and DLD-1 cells were transfected to express FLYWCH1 and TCF4. **B,** β-catenin-ChIP coupled with qPCR was used to quantify binding of FLYWCH1/β-catenin versus TCF4/β-catenin to the *c-jun* promoter, as outlined in **(A)**, using real-time PCR. Data are mean ± SD (n = 3; *, $P < 0.05$; **, $P < 0.01$; ***, $P < 0.001$). **C,** Western-blotting analysis of mock vs treated Wnt3a+R-spondin 1 in HCT116 cells after 24 hrs using the indicated antibodies. **D, E,** SW480 and DLD-1 cell-lines were treated with

Wnt3a+R-spondin1 conditional media or mock after 24 hrs. RNA was extracted and *FLYWCH*1-mRNA expression was assessed by real time qRT-PCR **(D)** and standard RT-PCR (N=3, 100bp marker was used) **(E)**. Data are mean ± SD (n = 6; **, P < 0.01). **F,** Levels of cyclin D1/D2 gene expression associated with the activation of Wnt signaling altered FLYWCH1 gene expression levels in SW480 cells using WB assays. SW480 cells were transfected to express FLYWCH1 (lanes 3 and 4) and control GFP (lanes 1 and 2).

Figure 4. FLYWCH1 modulates cell adhesion and morphology

A, SW480 cells stably expressing GFP (upper panel, control), transiently transfected with GFP-FLYWCH1 (middle panel), or stably expressing GFP-FLYWCH1-shRNA (lower panel). These cells were stained with Phalloidin and visualized under fluorescent microscope. Selected GFP expressing cells are boxed and magnified by the right far panel for each condition. Scale bars, 50 μm. **B,** Percentage of wound closure of GFP-FACS-sorted SW480 cells expressing GFP (control, blue), GFP-FLYWCH1 (green), or GFP-FLYWCH1-shRNA (red), following a scratch wound assay. Wound closure was measured at time zero (T0), 24hours (T24) and 48hrs (T48) as indicated. Data are mean ± SD (n = 6; *, P < 0.05; **, P < 0.01; ***, P < 0.001). Representative images are shown in Figure S3. **C,** The impedance, reflecting cell adhesion and spreading, was measured for GFP-FACS-sorted SW480 cells expressing GFP (control, blue), GFP-FLYWCH1 (green), or GFP-FLYWCH1-shRNA (orange) using Electric Cell-substrate Impedance Sensing (ECIS), over 30hrs. Data shows mean of duplicate wells of representative ECIS plates). The majority of GFP-FLYWCH1$^{O/E}$ cells were attached in 2-3hrs and cell spreading was readily detected by an impedance increase (c-left graph), compared with GFP (control) and FLYWCH1^{shRNA} cells.

Figure 5. FLYWCH1 regulates certain β-catenin/TCF4 target genes involved in the invasion

A, Bivariate scatter plot showing the distribution of up and downregulated 84 *WNT*-associated genes from SW480 cells expressing GFP-FLYWCH1 (experimental) vs GFP (control) using the human WNT- RT² profiler™ PCR array. Expression was determined by qRT-PCR. Down-regulated genes (blue), and up-regulated genes (yellow). **B,** The mRNA expression (left panel) and Western-blotting analysis of several tumourigenic and proinavsive β-catenin/TCF4 target genes in SW480 cells expressing GFP-FLYWCH1 (blue) and GFP-FLYWCH1-shRNA (red) relatively to the control cells expressing GFP (blank). Data are mean ± SD (n = 3; *, $P < 0.05$; **, $P < 0.01$; ***, $P < 0.001$). **C,** Western blot analysis of EMT markers and/or regulatory factors in SW480 cell lysate using the indicated constructs and antibodies. **D,** Effect of FLYWCH1 on ZEB1 transcription activity mediated by β-catenin/TCF4. Data are mean ± SD (n = 6; * or ^{o}, $P < 0.05$; ** or ^{oo}, $P < 0.01$; *** or ^{ooo}, $P < 0.001$). **E,** Effect of FLYWCH1 on ZEB1-promoter activity and transcription.

Figure 6. Low *FLYWCH*1-mRNA expression significantly associated with advanced tumours

A, Upper panel shows photomicrographs of CRC-TMA specimens analysed by ISH using a specific *FLYWCH*1 probe with strong (left panel), moderate (middle panel) and weak (right panel) expression. The lower panel shows a correlation between *FLYWCH*1 expression and tumour staging. Weak expression of *FLYWCH*1 is associated with more advanced stage of a tumour. N/A: samples were not available on slides after staining and perhaps wiped off through the ISH process. Scale bars; 50μm. **B,** qRT-PCR analysis of *FLYWCH*1, *EPHA*4 and *ZEB*1 mRNA expression in a cohort of thirty-three; normal, primary and metastatic tumour tissues from patients in Nottingham, UK, normalized to HPRT. Data are mean ± SEM (n = 3; *$p \leq .05$; **, $p \leq .01$). Experiments were performed in triplicate for each sample and repeated

on two independent occasions. **C,** Schematic representation shows the adverse effect of FLYWCH1 on cancer cell migratory potentials through inhibition of β-catenin signalling pathway.

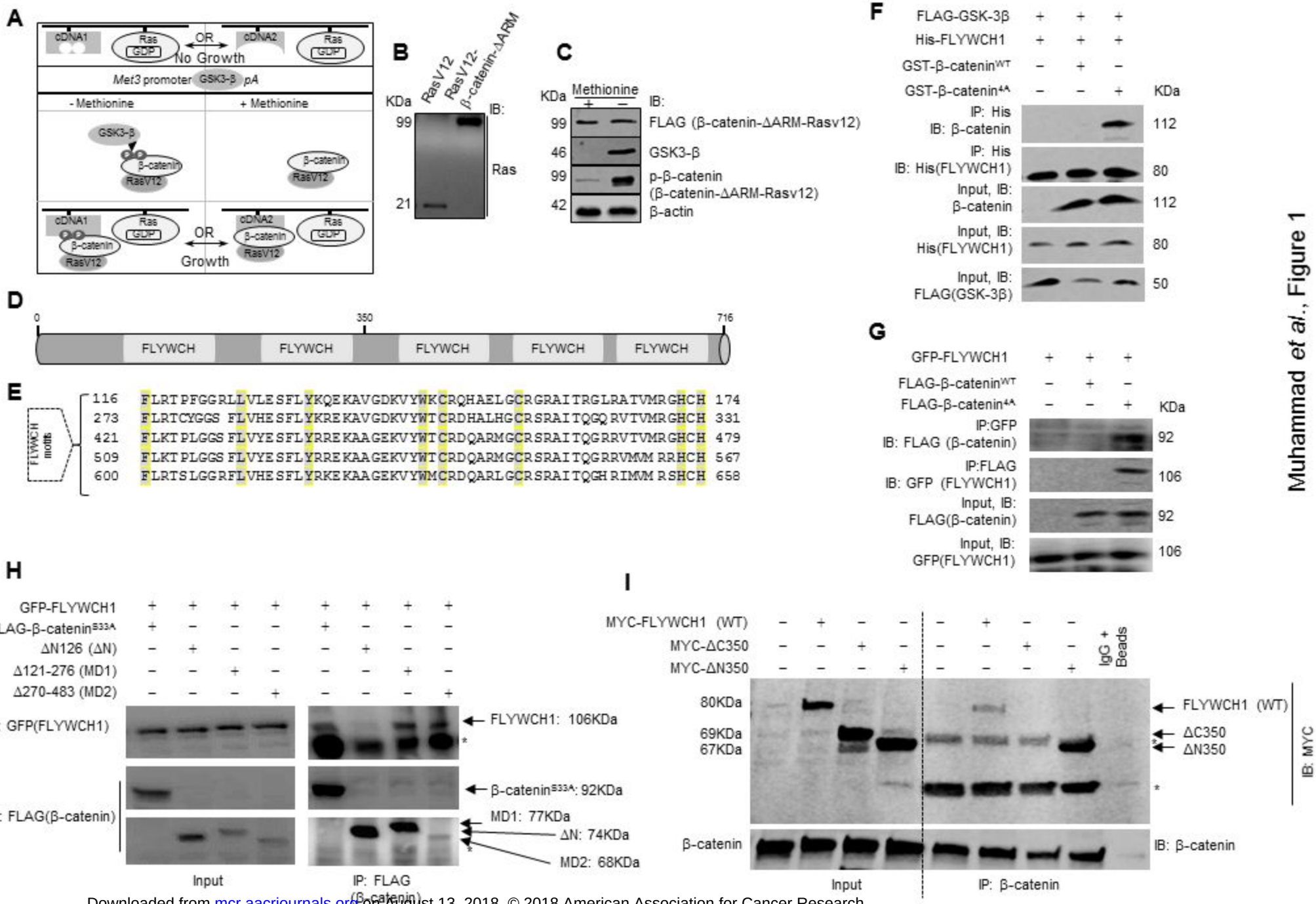

Muhammad *et al.*, Figure 1

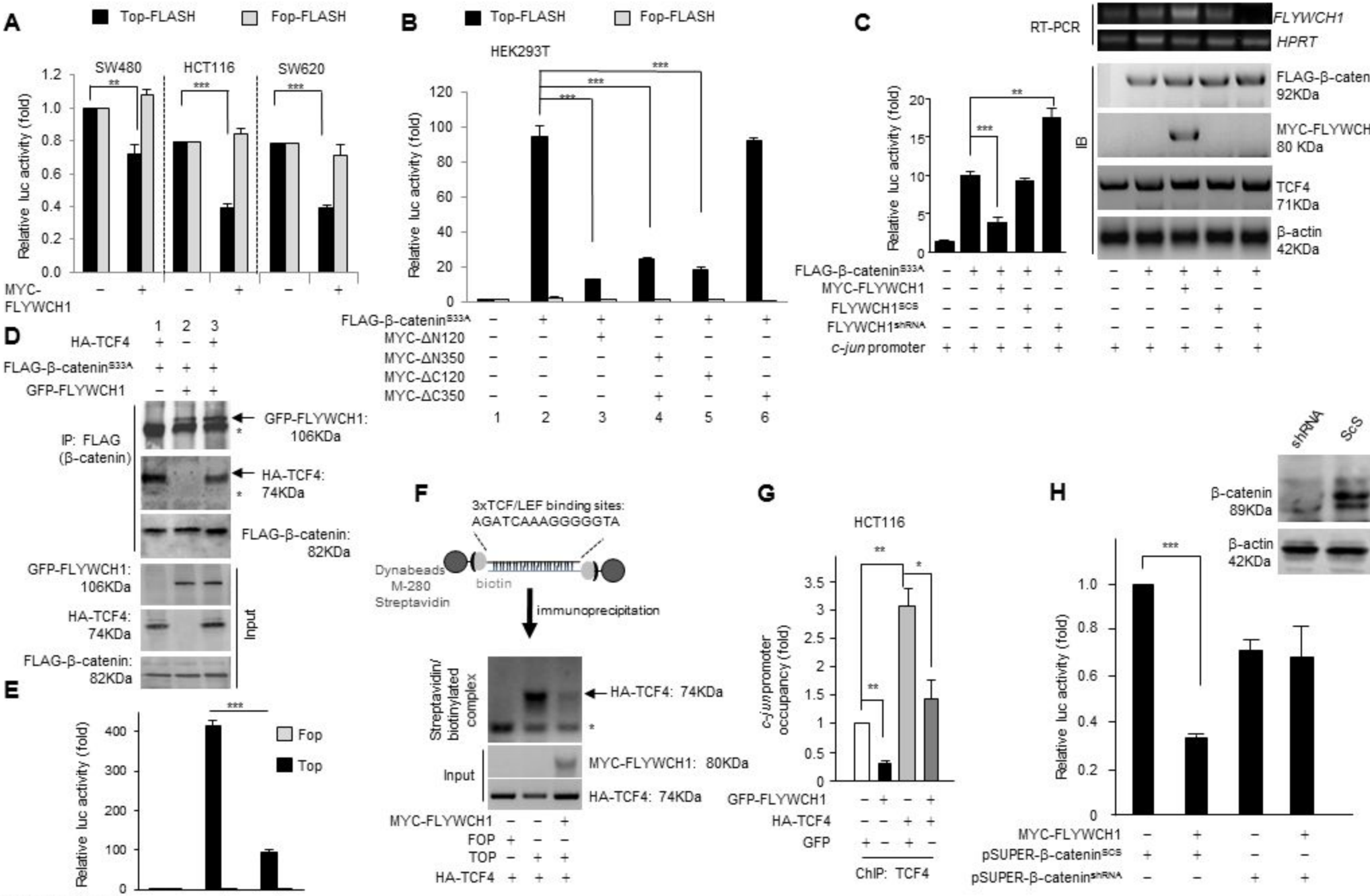

Muhammad *et al.*, Figure 2

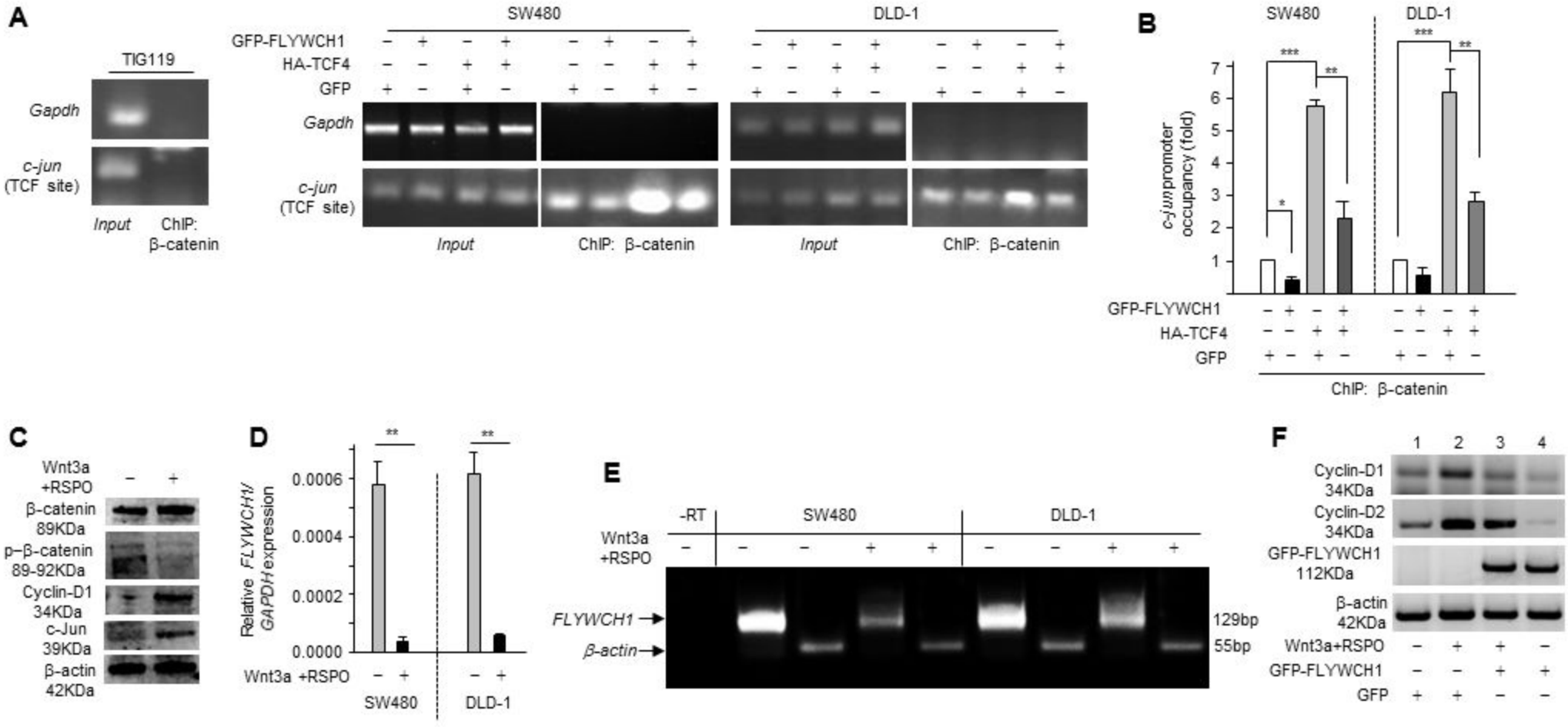

Muhammad *et al.*, Figure 3

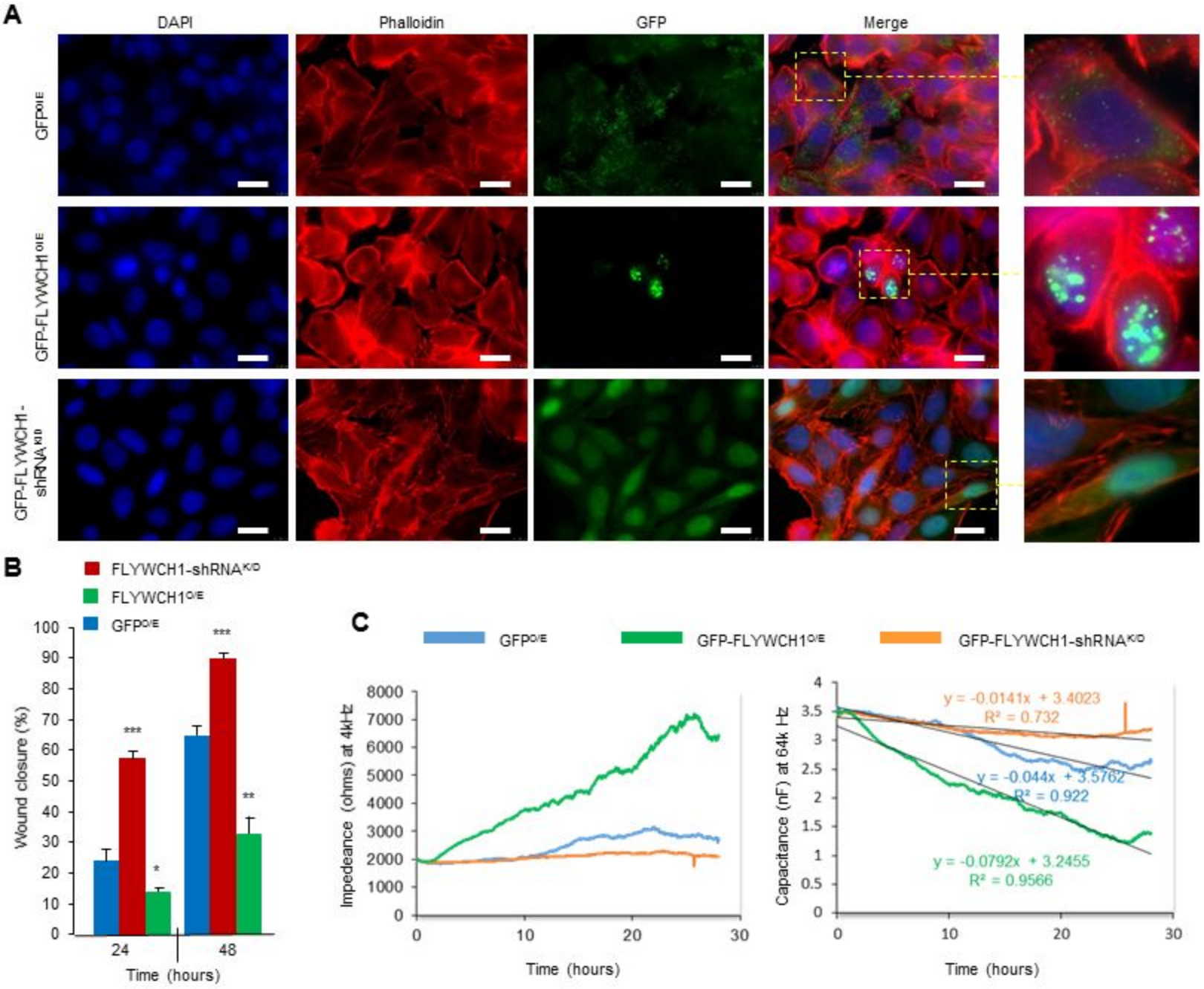

Muhammad et al., Figure 4

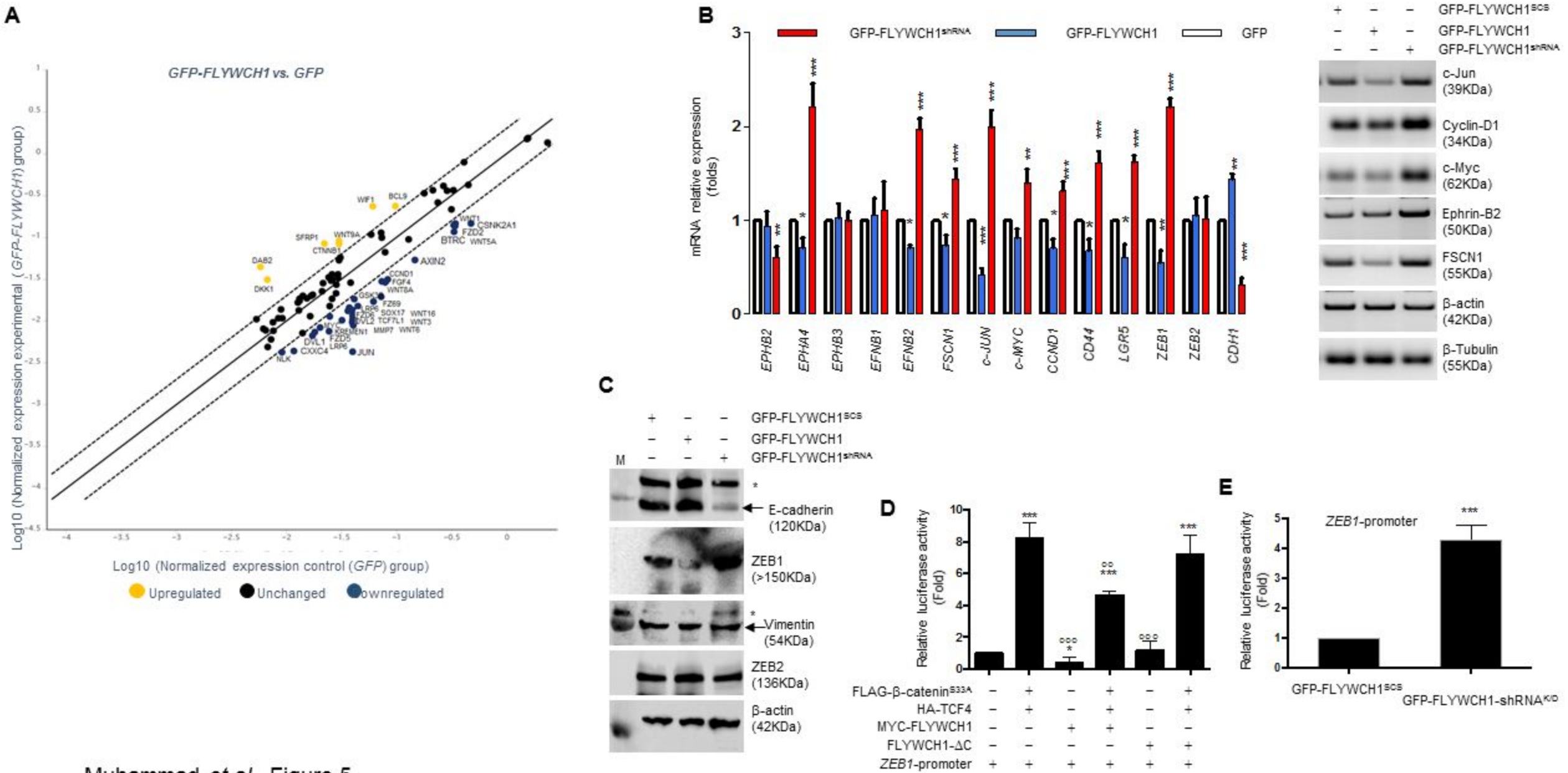

Muhammad *et al.*, Figure 5

A

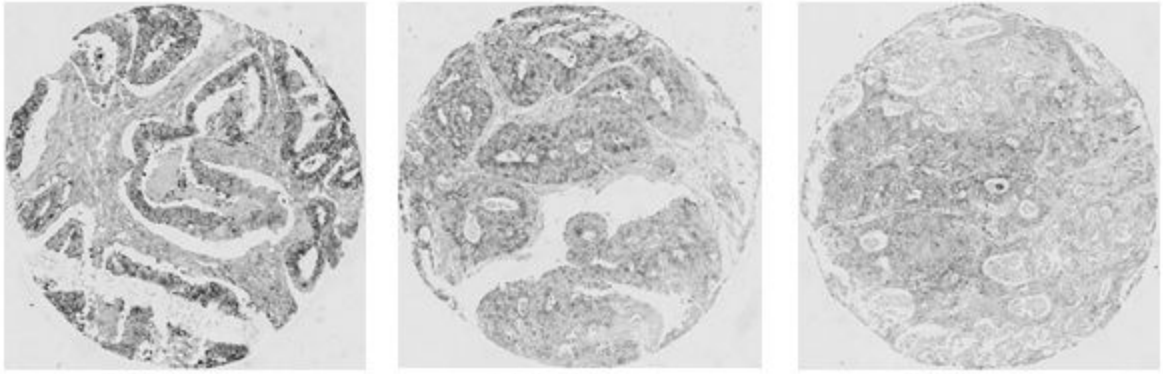

Tumour type	Total	N/A	Stained	ISH			
				High	Medium	Not detectable	Staining
				Strong	Moderate	Weak	Intensity
Early tumour	73	3	70 (100%)	23 (32.8%)	29 (41.4%)	18 (25.7%)	
Advanced tumour/ Metastatic	74	2	72 (100%)	8 (11.1%)	15 (20.8%)	51 (70.8%)	

B

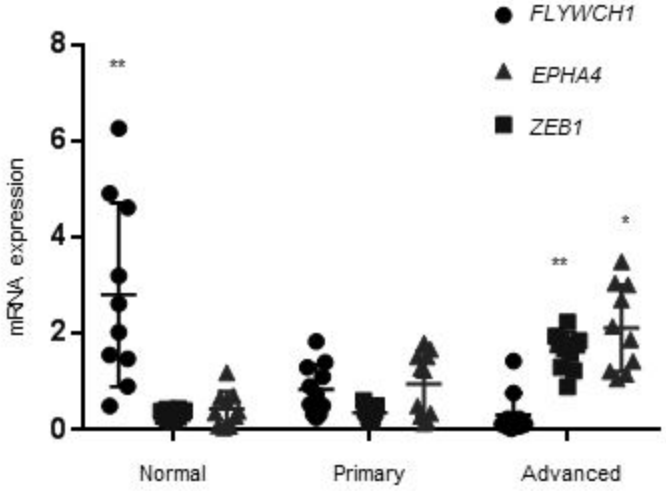

C

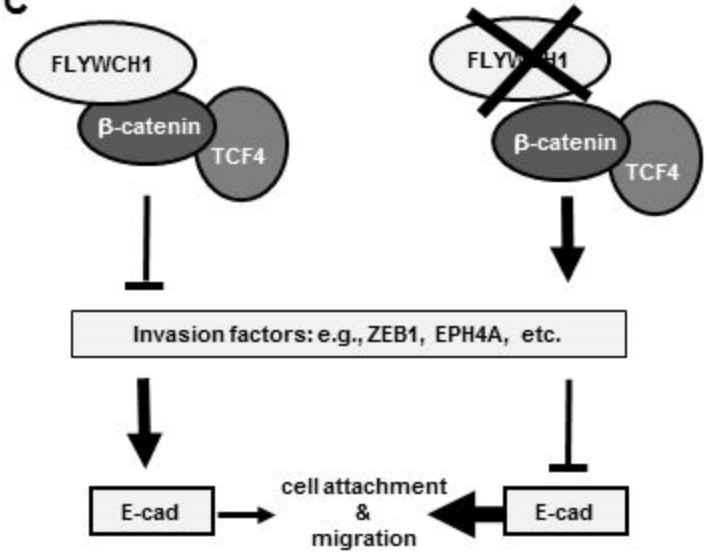

Muhammad *et al.*, Figure 6

AACR American Association for Cancer Research

Molecular Cancer Research

FLYWCH1, a Novel Suppressor of Nuclear β-catenin, Regulates Migration and Morphology in Colorectal Cancer

Belal A. Muhammad, Sheema Almozyan, Roya Babaei-Jadidi, et al.

Mol Cancer Res Published OnlineFirst August 10, 2018.